Title

Whole Brain Magnetic Resonance Spectroscopic Determinants of Functional Outcomes in Pediatric Moderate/Severe Traumatic Brain Injury.

Journal

Journal of neurotrauma, 35(14)

ISSN

0897-7151

Authors

Babikian, Talin
Alger, Jeffry R
Ellis-Blied, Monica U
et al.

Publication Date

2018-07-01

DOI

10.1089/neu.2017.5366

Peer reviewed

JOURNAL OF NEUROTRAUMA 35:1637–1645 (July 15, 2018)

DOI: 10.1089/neu.2017.5366

Whole Brain Magnetic Resonance Spectroscopic Determinants of Functional Outcomes in Pediatric Moderate/Severe Traumatic Brain Injury

Talin Babikian,[1] Jeffry R. Alger,[2] Monica U. Ellis-Blied,[3] Christopher C. Giza,[4] Emily Dennis,[5] Alexander Olsen,[6] Richard Mink,[7] Christopher Babbitt,[8] Jeff Johnson,[9] Paul M. Thompson,[10] and Robert F. Asarnow[11]

Abstract

Diffuse axonal injury contributes to the long-term functional morbidity observed after pediatric moderate/severe traumatic brain injury (msTBI). Whole-brain proton magnetic resonance echo-planar spectroscopic imaging was used to measure the neurometabolite levels in the brain to delineate the course of disruption/repair during the first year post-msTBI. The association between metabolite biomarkers and functional measures (cognitive functioning and corpus callosum [CC] function assessed by interhemispheric transfer time [IHTT] using an event related potential paradigm) was also explored. Pediatric patients with msTBI underwent assessments at two times (post-acutely at a mean of three months post-injury, $n=31$, and chronically at a mean of 16 months post-injury, $n=24$). Healthy controls also underwent two evaluations, approximately 12 months apart. Post-acutely, in patients with msTBI, there were elevations in choline (Cho; marker for inflammation and/or altered membrane metabolism) in all four brain lobes and the CC and decreases in N-acetylaspartate (NAA; marker for neuronal and axonal integrity) in the CC compared with controls, all of which normalized by the chronic time point. Subgroups of TBI showed variable patterns chronically. Patients with slow IHTT had lower lobar Cho chronically than those with normal IHTT; they also did not show normalization in CC NAA whereas those with normal IHTT showed significantly higher levels of CC NAA relative to controls. In the normal IHTT group only, chronic CC Cho and NAA together explained 70% of the variance in long-term cognitive functioning. MR based whole brain metabolic evaluations show different patterns of neurochemistry after msTBI in two subgroups with different outcomes. There is a dynamic relationship between prolonged inflammatory responses to brain damage, reparative processes/remyelination, and subsequent neurobehavioral outcomes. Multimodal studies allow us to test hypotheses about degenerative and reparative processes in patient groups that have divergent functional outcome, with the ultimate goal of developing targeted therapeutic agents.

Keywords: cognition; MK spectroscopy; neuropsychology; pediatric brain injury

[1]Department of Psychiatry and Biobehavioral Sciences, Semel Institute for Neuroscience and Human Behavior, Mattel Children's Hospital at UCLA, and the UCLA Steve Tisch BrainSPORT Program, Los Angeles, California.
[2]NeuroSpectroScopics, LLC, Sherman Oaks, California.
[3]Health Promotion and Disease Prevention Program, VA Loma Linda Healthcare System, Redlands, California.
[4]UCLA Brain Injury Research Center, Department of Neurosurgery, and Division of Pediatric Neurology, Mattel Children's Hospital, UCLA Steve Tisch BrainSPORT Program, Los Angeles, California.
[5]Imaging Genetics Center, Mark and Mary Stevens Neuroimaging and Informatics Institute, Keck School of Medicine, University of Southern California, Marina del Rey, California.
[6]Department of Psychology, Norwegian University of Science and Technology, Trondheim, Norway; Department of Physical Medicine and Rehabilitation, St. Olavs Hospital, Trondheim University Hospital, Trondheim, Norway.
[7]Pediatric Critical Care Medicine, Harbor-UCLA Medical Center; Los Angeles BioMedical Research Institute, Department of Pediatrics, Torrance, California.
[8]Miller Children's and Women's Hospital of Long Beach, Long Beach, California.
[9]LAC+USC Medical Center, Department of Pediatrics, Los Angeles, California.
[10]Imaging Genetics Center, Mary and Mark Stevens Institute for Neuroimaging and Informatics, Keck School of Medicine, University of Southern California, Marina del Rey, California; Departments of Neurology, Pediatrics, Psychiatry, Radiology, Engineering, and Ophthalmology, USC, Los Angeles, California.
[11]Departments of Psychology and Psychiatry and Brain Research Institute, David Geffen School of Medicine, Los Angeles, California.

Introduction

Moderate/severe traumatic brain injury (msTBI) experienced in childhood is one of the leading causes of neurologic-based functional morbidity in childhood in the United States and worldwide.[1] Diffuse (multifocal) axonal injuries (DAI), which disrupt the white matter connections in the brain, are very common in these types of injuries.[2] This is relevant especially in childhood, because the brain is in a period of rapid growth and myelination, and any disruptions to this process in the course of normal development can have chronic consequences in cognitive, health, social, and emotional outcomes.[3,4]

In addition to structural changes identified by diffusion tensor and related imaging technology,[5–9] the neurometabolic cascade including physiologic, ionic, and metabolic changes initiated by msTBI can cause secondary damage. The resulting functional morbidity can vary in time course and nature, depending on injury severity. Magnetic resonance spectroscopy (MRS) provides noninvasive quantitative metabolite measures that complement measures of structural change.

One of the most studied metabolites in neurological disorders, including msTBI, is N-acetylaspartate (NAA), because it can be measured noninvasively with MRS. NAA is a robust marker of both neuronal and axonal integrity,[10] plays an important role in oligodendrocytes and myelin production,[11,12] and is a marker of mitochondrial dysfunction.[12] Reductions or alternations in MRS-measured NAA may reflect ongoing mitochondrial dysfunction, loss of viable neurons, or disruption in myelination.[12]

MRS studies in TBI have also focused on choline (Cho) containing compounds, which are precursors and catabolytes of the phospholipids that form cell/organelle membranes and myelin membranes, although the MRS-derived Cho signal is more likely to measure free Cho, glycerophosphorylcholine, and phosphorylcholine. Whereas decreased Cho can reflect cell loss, increased Cho can signify membrane turnover, cellular proliferation, and/or gliosis.[10,12] Other metabolites of interest that produce quantifiable MRS signals have included creatine (Cre), which can also be an indicator of cellular function and dysfunction.[13–15]

Using single voxel or single slice MRS methods, previous research has shown that in acute pediatric msTBI, there are reductions in NAA and elevations in Cho, which correlate with later neurologic and neuropsychological outcome.[13,16] Similar neurometabolic alterations have been reported at longer post-injury times,[17] with correlations observed with neuropsychological and behavioral functioning.[18–20] Advances in imaging technology recently have made whole brain three dimensional (3D)-MRS imaging (MRSI) acquisition possible. In adult patients with TBI of varying injury severities, whole brain 3D-MRSI studies have shown widespread alterations in Cho and NAA, that are correlated with injury severity and neuropsychological functioning.[21–23] No studies, however, have used whole brain 3D-MRSI to evaluate a sample of pediatric patients or evaluated its relationship with functional outcomes.

We found recently that event-related potential (ERP)-based interhemispheric transfer time (IHTT) assessed during the post-acute period may be a valuable biomarker in subgrouping children with msTBI into those who appear more adversely affected by their injury, defined by poor cognitive functioning, and progressive abnormalities in white matter organization.[24–26] We extend those findings in this article by evaluating the neurometabolic status of the subgroups of msTBI defined by IHTT and healthy controls to determine whether neurometabolic abnormalities can explain further the white matter pathophysiology that underlies neurobehavioral morbidity observed in children with slow IHTT post-msTBI.

We applied whole brain MRS technology to characterize the metabolite levels in brain structures sensitive to msTBI (lobes, corpus callosum [CC], hippocampus, and cerebellum) at two discrete times, post-acutely (when the brain is still in a state of recovery) and again at approximately 16 months post-injury (when a substantial degree of repair and recovery has occurred) to delineate the course of disruption and repair during the first year after pediatric msTBI.

Methods

Subjects

Patients recruited from four pediatric intensive care units located in Level 1 trauma centers who met Glasgow Coma Scale (GCS) criteria for moderate to severe brain injury (intake or post-resuscitation GCS score between 3 and 12, or higher GCS with confirmed abnormalities on clinical imaging), were 8–18 years old at injury and did not have significant pre-trauma histories of psychiatric or neurologic morbidity. Of the children who enrolled in the overall study, 31 underwent MRSI post-acutely and 24 underwent MRSI chronically, whose data are reported in this article.

ERP IHTT was used to divide the msTBI group into subgroups, per the methods described in our previous article.[24] In short, the TBI subgroup labeled ''slow IHTT'' had an IHTT lower than the IHTT of the healthy control group by 1.5 standard deviations. Those within 1.5 standard deviations of the mean IHTT of the control group were labeled ''normal IHTT.'' In addition, 48 demographically matched healthy controls were also enrolled. Demographic and other subject details are presented in Table 1.

Neurocognitive measures

The functional domains assessed included intellectual functioning, verbal memory, psychomotor skills, working memory, and inhibition/set-switching using standardized measures. All of the above standardized scores, were combined into a single cognitive performance index, the psychometric details of which are described in detail elsewhere.[27]

IHTT from ERP paradigm

Visual ERPs were used to measure IHTT, defined as the time required to transfer stimulus-locked neural activity between the left and right brain hemispheres in the participants. Electroencephalography was recorded while participants completed a computerized, pattern-matching task with bilateral field advantage. The cross-callosal IHTT of each participant was calculated using the electroencephalographic visual ERPs, which were collected during the unilateral conditions. Greater detail on this method has been described previously[28] and in our own work with these subjects.[24]

Brain imaging acquisition

Participants were scanned on 3T Siemens Trio MRI scanners (Siemens Healthcare GmbH, Germany). T1-weighted 3D images were acquired with magnetization prepared rapid gradient echo imaging (MPRAGE) using the following acquisition parameters: GRAPPA mode; acceleration factor phase encoding (PE) = 2; repetition time (TR)/echo time (TE)/T1 = 1900/3.26/900 msec; field of view (FOV) = 250×250 mm^2; an axial plane acquisition with isotropic voxel size = 1 mm, flip angle = nine degrees. A 12-channel head coil was used.

Partway through the study, scanning moved from the UCLA Brain Mapping Center (BMC) to the Staglin IMHRO Center for

Table 1. Subject Characteristics by Group, Means (Standard Deviation)

	msTBI		
	Slow IHTT	*Normal IHTT*	*Healthy controls*
N: Post-acute	14	17	48
Chronic	12	12	35
Age at first testing (years)	14.0 (2.5)	14.3 (3.3)	15.6 (2.7)
Sex (% female)	36%	24%	52%
Time since injury (weeks): Post-acute	11.6 (4.2)	12.6 (5.5)	N/A
Chronic	63.7 (7.8)	69.5 (8.0)	N/A
GCS: At admission	8.9 (3.6)	8.2 (3.9)	N/A
Lowest in 24 h	7.0 (3.6)	8.3 (4.0)	N/A
Parent education (years)	13.0 (3.7)	14.4 (3.7)	15.1 (3.6)
IHTT (msec)	26.0 (6.6)*^	7.9 (5.8)^	9.4 (5.8)*
Performance index: Post-acute	90.4 (12.6)*	98.6 (12.0)	104.0 (10.4)*
Chronic	93.8 (12.2)*	102.3 (13.4)	110.9 (10.3)*

TBI, traumatic brain injury; IHTT, interhemispheric transfer time; GCS, Glasgow Coma Scale.
* or ^ Pairwise difference significant at $p < 0.05$.

Cognitive Neuroscience (Staglin). Both scanners were 3T Siemens Trio scanners, and the protocol was maintained. To determine that scanner change did not introduce bias into our data, we scanned six healthy adult volunteers at both the BMC and Staglin centers, 1.5 months apart. We then assessed possible scanner effects based on the T1-weighted image pairs. Extensive details of this process can be found in our previous article.[8]

MRSI data were obtained using a volumetric spin-echo EPSI sequence (TR/TE = 1710 msec/70 msec, FOV: $280 \times 280 \times 180$ mm^3, 100 [read] $\times$ 50 [phase] $\times$ 18 [slice] spatial samples over a 135-mm slab, and acquisition time of 26 min). This method has been validated and used previously in a number of publications.[23,29] It included frequency-selective water suppression and inversion-recovery nulling of the lipid signal with T1 = 198 msec. This pulse sequence included both a spin-echo excitation for the metabolite signals and a low flip-angle gradient-echo acquisition of a water reference signal, which was acquired in an interleaved fashion.

The MPRAGE MRI and MRSI acquisitions were performed at the same angulation, with the slice or slab orientations of all acquisitions parallel to the anterior commissure-posterior commissure (AC-PC) plane, or angulated at +15 degrees from the AC-PC, which was found to facilitate improved magnetic field homogeneity over a larger volume of the cerebrum. Figure 1 illustrates the general MRSI quality with data taken from a single spectroscopic imaging slice from a single subject with brain injury. Figure 2 illustrates that the MRSI method produces multiple slices allowing study of almost the entire brain.

MRSI data were processed in a fully automated manner using the MIDAS package, the details of which can be found in previous publications.[23–30] The processing steps included calculation of the MRSI voxel tissue content based on tissue segmentation of the high-resolution T1-weighted MRI; signal normalization to institutional units using the water reference data; and spatial registration to the simulated Montreal Neurological Institute MRI template,[31] which was matched to a brain atlas that delineated the eight hemispheric lobes and the cerebellum.[32] Absolute voxel levels of NAA, Cr, and Cho were obtained for all four lobes, right and left hemisphere separately. In addition, metabolite levels for the right and left hemisphere cerebellum, hippocampus, as well as the body, genu, and the splenium of the CC were also derived.

Results

General linear models (GLM) and analyses of variance (ANOVAs) were used to identify group differences in individual and combined brain regions, respectively. Pearson correlations were used to assess associations between pairs of variables, and linear regression models were used to identify proportion of variance explained by predictor variables. Data were evaluated for parametric properties for the utilization of the above methods. There were no between-group and within-group differences in the right and left hemisphere measurements for either the post-acute or chronic data for any of the brain regions; therefore, hemispheric data were combined into individual structures (e.g., temporal lobe, etc.) for the analyses below. Further, there were no group differences in any of the regions for Cre. Therefore, no further analyses were performed with Cre.

Below, we present cross-sectional analyses of post-acute and chronic data. Note that the differences highlighted below between the groups in the post-acute versus chronic time points were remarkably similar when only the subgroup of patients who were seen at both time points were evaluated; therefore, only the cross-sectional data are presented below. Further, GCS (initial and lowest within 24 h) was not significantly correlated with any of the key metabolites explored in this article. Also, when the TBI group was separated into those with GCS in the traditionally defined moderate/severe range (3–12) versus those with GCS in the mild range (13–15) but who had positive imaging findings and thus needed intensive care intervention, there were no differences in any of the metabolite readings in the post-acute period for any of the key variables described below. Thus, we were comfortable in combining this ''complicated'' mild TBI group with our msTBI group.

Cross-sectional analyses

Between-group GLM results are reported in Table 2. For post-acute studies, *post hoc* (with Bonferroni corrections) analyses for Cho indicated that both TBI groups showed higher lobar Cho than the healthy control group, but that the TBI subgroups were not significantly different from one another. The normal IHTT TBI group had higher Cho than the healthy control group in the body of the CC, and both TBI groups had higher Cho than the healthy control group in the splenium of the CC (all $p < 0.05$). No group differences in the hippocampal or cerebellar metabolic measurements were noted for Cho.

Post hoc analyses NAA showed that both TBI groups had lower NAA in the splenium than the healthy control group ($p < 0.01$) but

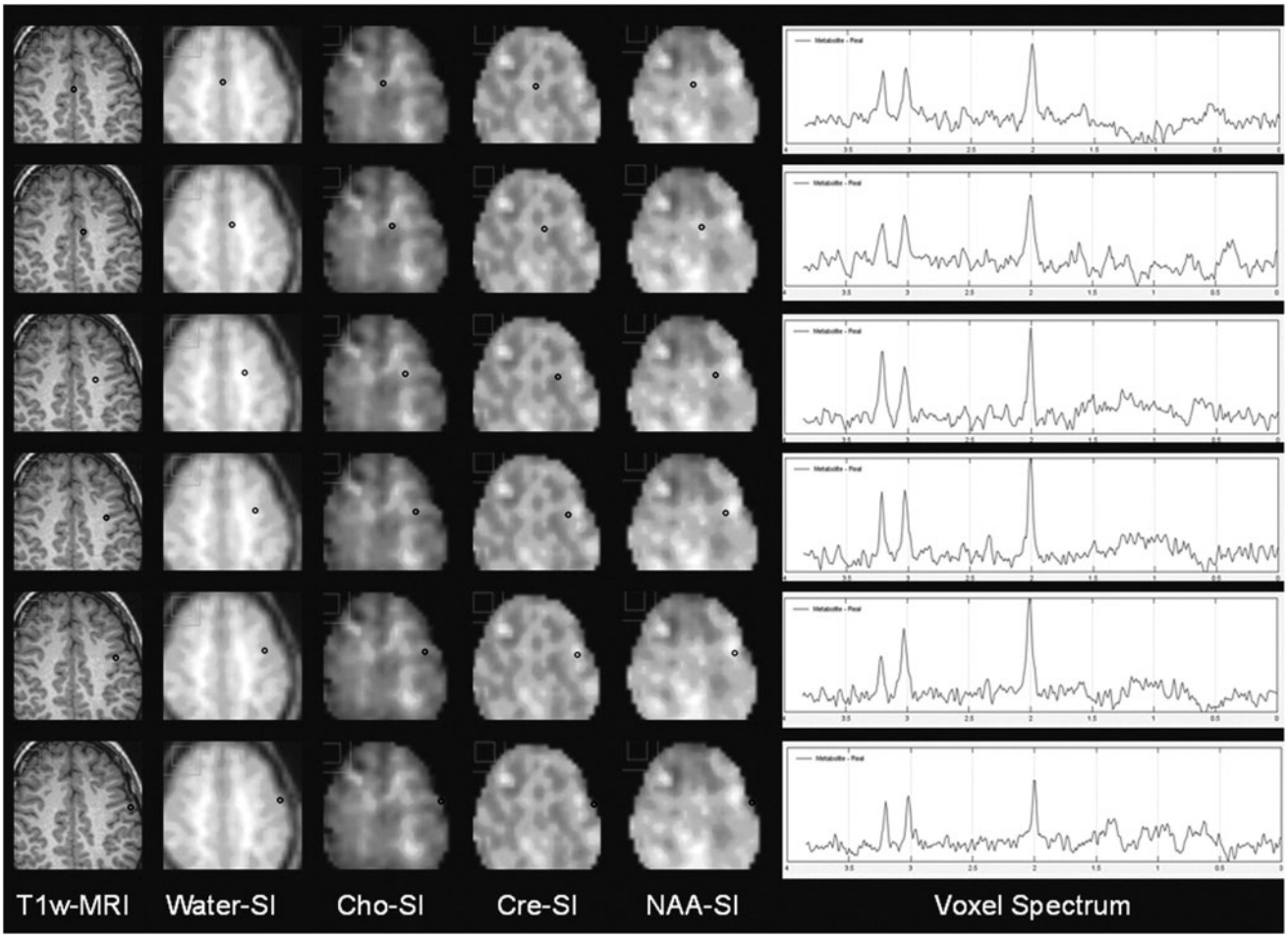

FIG. 1. This figure illustrates the general magnetic resonance spectroscopy imaging quality with data taken from a single spectroscopic imaging slice from a single subject with brain injury. Thirty-two such slices are produced in each study. The circles illustrate the nominal in plane voxel size (2.5 mm diameter) after spatial filtering and interpolation. Each row in the figure has the voxel position shifted two nominal voxel widths toward the subject's left (the images follow radiological convention). The leftmost column displays the T1-weighted (MPRAGE) image intensity aligned to the spectroscopic images of water, total choline (Cho), total creatine (Cre), total N-acetylaspartate (NAA). The rightmost column displays the voxel spectrum produced by the region identified by the circles. The voxel spectra illustrate the typical signal-to-noise ratio and spectral resolution. They also illustrate that in general for lipid signals produce no interference with the NAA signal within about 5 mm from the head surface. MRI, magnetic resonance imaging.

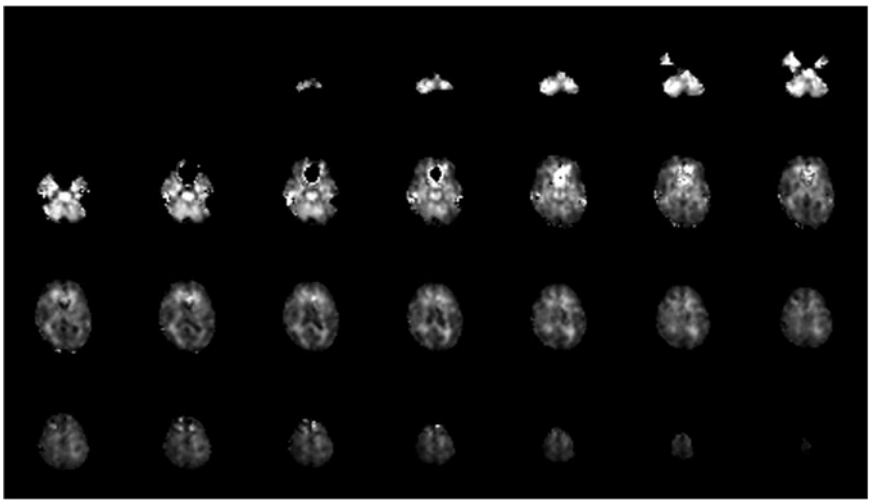

FIG. 2. This figure illustrates that the MRSI method produces multiple slices allowing study of almost the entire brain. The figure shows the total choline volume image from a single TBI subject in multi-slice format.

Table 2. General Linear Model Results for Individual Regions in Three Groups

	NAA		*Cho*	
Group	*Post-Acute*	*Chronic*	*Post-Acute*	*Chronic*
Temporal	ns	ns	$p<0.01$	ns
1	13890 (688)	13445 (321)	2426 (110)	2120 (77)
2	14908 (743)	14118 (347)	2426 (119)	2262 (83)
3	14179 (441)	13959 (206)	2160 (71)	2138 (49)
Parietal	ns	ns	$p<0.01$	$p<0.05$
1	13931 (543)	12589 (363)	2005 (88)	1734 (58)
2	14120 (587)	13955 (392)	2170 (95)	1914 (63)
3	13527 (349)	13433 (233)	1755 (57)	1775 (37)
Occipital	ns	ns	$p<0.01$	ns
1	14115 (617)	13592 (359)	1726 (96)	1529 (67)
2	14015 (667)	14388 (387)	1904 (104)	1649 (73)
3	14225 (396)	13739 (230)	1523 (62)	1515 (43)
Frontal	ns	ns	$p<0.01$	$p<0.05$
1	13537 (533)	12742 (326)	2304 (95)	2048 (61)
2	14489 (575)	14005 (352)	2554 (102)	2277 (66)
3	13425 (342)	13356 (209)	2045 (61)	2101 (39)
Body	ns	$p<0.05$	$p<0.05$	$p=0.06$
1	12934 (612)	12366 (724)	2566 (157)	2074 (512)
2	14925 (661)	16383 (782)	2903 (170)	3841 (553)
3	14233 (393)	14418 (464)	2416 (101)	2500 (329)
Genu	$p<0.05$	ns	ns	$p=0.06$
1	11253 (1007)	9927 (1234)	3294 (245)	2355 (606)
2	11086 (1087)	14675 (1333)	2949 (245)	4518 (655)
3	13441 (646)	12479 (792)	2689 (157)	2763 (389)
Splenium	$p<0.05$	ns	ns	$p=0.09$
1	13271 (413)	14664 (1870)	2495 (89)	1929 (961)
2	13553 (446)	19317 (2020)	2326 (96)	4580 (1038)
3	15135 (265)	14958 (1200)	2055 (57)	2013 (616)
Hippocampus	ns	ns	ns	ns
1	12756 (915)	16006 (1115)	2751 (222)	3328 (706)
2	14930 (988)	16269 (1205)	3108 (239)	4495 (763)
3	14917 (587)	14687 (716)	2884 (142)	2938 (453)
Cerebellum	$p<0.05$	$p<0.01$	ns	$p<0.01$
1	12669 (478)	12074 (563)	3228 (171)	2797 (175)
2	14456 (516)	13964 (609)	3499 (184)	3260 (189)
3	14317 (307)	14245 (362)	3541 (109)	3501 (112)

NAA, N-acetylaspartate; Cho, choline.

Group 1: Slow interhemispheric transfer time (IHTT) traumatic brain injury (TBI); Group 2: Normal IHTT TBI; Group 3: healthy control. Ns, overall general linear model not statistically significant. Means (in generic institutional values per Maudsley, 2006[30]) and standard deviations (in parentheses) for each metabolite by time point and by group. Statistically significant pairwise differences are discussed in the text section Combined Lobar and Combined CC Regions.

were not different from one another. In the genu, the normal IHTT TBI group had lower NAA than the healthy control group ($p<0.05$); and in the cerebellum, the slow IHTT TBI group had lower NAA than the healthy control group ($p<0.05$). All other differences were not statistically significant.

For chronic studies, *post hoc* analyses of Cho indicated that the normal IHTT TBI group had higher frontal and parietal Cho than the slow IHTT TBI group. The healthy control group had higher Cho in the cerebellum than the slow IHTT TBI group. For NAA, post-analyses showed that in the cerebellum, the slow IHTT TBI group had lower NAA than the normal IHTT or the healthy control group ($p<0.05$). In the body of the CC, the normal IHTT TBI group had higher NAA than the slow IHTT TBI group ($p<0.05$).

Combined lobar and combined CC regions

To minimize the number of analyses performed, and because certain regions performed similarly regarding group differences in NAA and Cho, metabolite data were combined (additive) for the lobar regions and the CC, resulting in a single metabolic measurement for lobar Cho, CC Cho, and CC NAA, the three regions in which group differences were consistently observed in the above analyses. Age at the time of assessment was not correlated with any of the metabolite measurements in either group and was, therefore, not considered in the following analyses.

At the post-acute time, ANOVA for the three groups (slow IHTT msTBI, normal IHTT msTBI, and healthy control) was significant for lobar Cho ($p<0.01$), CC Cho ($p=0.03$), and CC NAA

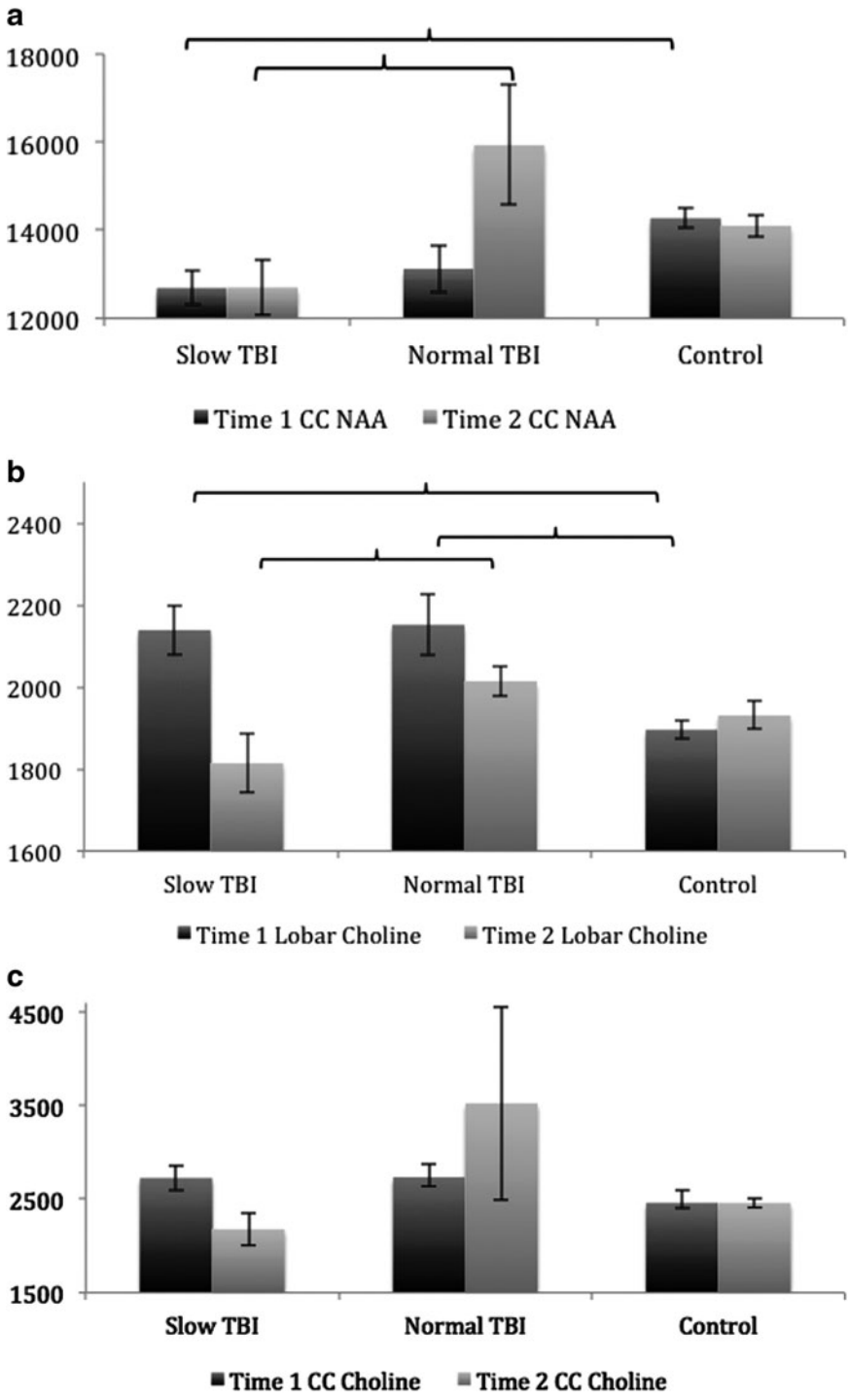

FIG. 3. Brackets indicate pairwise comparison differences significant at $p < 0.05$. Time 1: Post-Acute, Time 2: Chronic. Metabolite levels are based on institutional units, as defined in Maudsley (2006).[30] TBI, traumatic brain injury; CC, corpus callosum; NAA, N-acetylaspartate.

($p < 0.01$). *Post hoc* analyses (with Bonferroni corrections) showed that the slow IHTT msTBI group exhibited significantly lower CC NAA than the healthy control group ($p < 0.05$), but no other statistically significant differences were found (Fig. 3a). Both msTBI groups showed higher levels of lobar Cho than the healthy control group ($p < 0.05$), but did not differ from each other (Fig. 3b). Further, both TBI groups had slightly higher CC Cho than the healthy control group, but the differences were not statistically significant (Fig. 3c).

At the chronic time, a simple ANOVA showed significant group differences for lobar Cho ($p < 0.05$) and CC NAA ($p < 0.05$); no other significant group differences were apparent. *Post hoc* analyses showed that the slow IHTT msTBI group had lower lobar Cho ($p < 0.05$) and lower CC NAA than the normal IHTT msTBI

group ($p < 0.05$ for both) (Fig. 3a, 3b). Although the difference between CC NAA between the two TBI groups and the normal control group was not statistically significant, it was noteworthy that the normal IHTT msTBI group appeared to have ''over-corrected'' for the initial NAA loss as illustrated by a much higher mean CC NAA than the healthy control group (Fig. 3a).

Associations between key metabolites

Pearson bivariate correlations were explored for each of the TBI groups at each time point. Only in the slow IHTT msTBI group, there was a robust and significant negative correlation between post-acute CC NAA and chronic lobar Cho ($r = -0.965$, $p < 0.001$, R^2 Linear $= 0.93$). In both TBI groups (explored separately), chronic lobar Cho and chronic CC NAA were positively associated (slow IHTT TBI group: $r = 0.643$, $p = 0.045$, R^2 Linear $= 0.41$ and normal IHTT TBI group: $r = 0.723$, $p = 0.012$, R^2 Linear $= 0.52$).

Predictors of cognitive outcome

None of the metabolite readings at either time were correlated with cognition at a statistically significant level in the slow IHTT msTBI sample. In contrast, within the normal IHTT msTBI group, chronic CC Cho and chronic CC NAA measurements were negatively correlated significantly with cognition at the post-acute time point (Cho: $r = -0.642$, $p = 0.045$ and NAA: $r = -0.637$, $p = 0.047$) and cognition at the chronic time point (Cho: $r = -0.880$, $p = 0.002$ and NAA: $r = -0.779$, $p = 0.013$).

In a linear regression model, neither post-acute nor chronic metabolite levels were predictive of short (post-acute) or long-term (chronic) cognitive performance in the slow IHTT msTBI group. In the normal IHTT msTBI group, however, only post-acute CC NAA was marginally predictive of post-acute cognition ($p = 0.06$, adjusted $R^2 = 19\%$), with no other significant associations observed. Cognitive performance at the chronic time point, again in the normal IHTT msTBI group, was significantly predicted by both chronic CC NAA and chronic CC Cho, together explaining 70% of the variance (adjusted R^2) in chronic cognition ($p = 0.01$).

Discussion

This is the first study to examine whole brain proton MRS at multiple timepoints (post-acute and chronic assessments) in pediatric patients with modest to severe TBI and its relation to neurobehavioral correlates. We identified robust group differences in Cho in the lobes and the CC, as well as NAA in the CC regions in our msTBI versus healthy control group analyses, and thus created mean composites for lobar Cho, CC NAA, and CC Cho that were used in subsequent analyses. In previous studies in this sample, we found that a visual ERP measure identified two subgroups of children who differed significantly in the course of brain structure and function in the 18 months after msTBI. In the current study, the two subgroups of msTBI children differed in their levels of NAA and Cho over time.

In the post-acute period, both msTBI groups showed elevations in lobar Cho, a marker for cell/membrane damage in the acute period, relative to the healthy control group. At the chronic timepoint, the more greatly impaired slow IHTT group showed lower Cho compared with the normal IHTT msTBI group. The Cho signal at this chronic time point may reflect membrane synthesis/turnover as part of continued recovery or inflammation/gliosis. Elevations in Cho can have different meanings at different times post-injury.

Elevated Cho may not always predict more impairment or poorer outcome, as previously assumed and reported.[6,18] Initial (post-acute) elevations in Cho may be indicators of cellular/membrane damage, which would explain its prognostic value as a marker of poor outcome[6,16]; however, Cho levels in the chronic timepoint might represent ongoing proliferation and repair processes in the form of membrane synthesis/turnover or gliosis. At the chronic time point, levels of Cho that are too low may suggest cell death or lack of healthy turnover or repair, as may be the case in the subgroup of msTBI patients who showed slow IHTT.

Also of note, the presence of Cho abnormalities in the peripheral brain regions (lobes) rather than only in the white matter tracts suggests that the underlying pathophysiology represented by this metabolite is a global brain phenomenon and perhaps indicative of pathology other than demyelination. Finally, Cho was not a significant predictor of cognition in the slow IHTT group, but chronic Cho was correlated with both post-acute and chronic cognition in the normal IHTT group.

In contrast to the global Cho findings in the brain, alterations (decreases) in NAA were restricted primarily to white matter tracts—namely, segments within the CC. Post-acutely, CC NAA was lower in the two msTBI subgroups relative to the healthy control group, although more so in the slow IHTT subgroup, and did not recover in the first year post-injury in this subgroup. On the other hand, CC NAA in the subgroup of msTBI patients with normal IHTT not only recovered but also ''overshot'' the mean of the healthy control group in the subgroup of msTBI patients with normal IHTT. Therefore, the subgroup of msTBI patients who showed the best brain function (based on their healthy IHTT) also had a higher mean CC NAA at the chronic time point.

Taken together, our findings suggest that in the msTBI subsample with impairments in brain function (slow IHTT) and disruption of white matter microstructural organization,[8,26] there is initial neuronal loss (demonstrated by low NAA) and impairment in oligodendrocyte/myelin function, which does not normalize over time. There is also evidence of increased membrane turnover or breakdown, which does not continue at the chronic timepoint. The latter findings suggest that after msTBI, the slow IHTT subgroup of patients does not show the neurometabolic signs of repair and recovery.

In contrast, the normal IHTT subgroup of msTBI patients shows a similar pattern of metabolic disruptions as the slow IHTT group initially, but by the chronic time point, a different metabolic profile emerges. In the normal IHTT group at the chronic time point, there are elevations in NAA in the CC and continued elevation in both lobar Cho and CC Cho (although less pronounced in the latter), suggesting ongoing remyelination, cellular proliferation, and membrane repair/turnover that is ongoing. In both subgroups, lobar Cho and CC NAA levels were highly (positively) correlated. Interestingly, only in the slow IHTT msTBI group, was there a robust negative correlation between post-acute CC NAA and chronic lobar Cho, further supporting the notion that the Cho signal is important in prognosis, but its interpretation as an indicator of positive or negative outcomes varies based on the time of the post-injury reading and its relation to other metabolites.

The limitations of this study include its relatively small sample size, especially after the subgrouping of the msTBI sample, which did not allow us to form more conclusive opinions on the findings or conduct more elegant modeling to more definitively form conclusions. Also, it appears that by our post-acute period, underlying biological processes have already occurred. To elucidate the pathophysiology contributing to the divergence we identified two to four months post-injury, evaluations at earlier time points than we have would be necessary.

Our findings are based on a relatively small sample but provide compelling evidence of differences in the metabolic profiles of the two subgroups of patients with msTBI with slow and normal IHTT identified in our previous studies. The physiological process reported by Cho and NAA may vary depending on the time post-injury, and the dynamic relationship between metabolites over time suggests that the brain is still responding to an msTBI even after the first year of injury. Ongoing longitudinal studies at distinct times along with whole brain analyses of metabolites will continue to help researchers understand the dynamic and interrelated associations, and along with multi-modal structural studies (e.g., diffusion tensor imaging) help further elucidate pathobiological factors that predict long-term outcomes. Doing so will allow us to identify biological therapeutic targets (genetic and/or pharmaceutical) to improve outcomes in this heterogeneous clinical population.

Acknowledgments

This work was supported in part by: R01HD061504; R01NS 27544; R01NS072308; K99NS096116; U54EB020403; R01AG 040060; R01NS080655; UCLA Brain Injury Research Center; UCLA Faculty Research Grant; UCLA Steve Tisch BrainSPORT Program. We thank the families who participated, and for our research coordinators Alma Martinez and Alma Ramirez, who diligently worked to ensure the success of this project.

Author Disclosure Statement

No competing financial interests exist.

References

1. Nguyen, R., Fiest, K.M., McChesney, J., Kwon, C.S., Jette, N., Frolkis, A.D., Atta, C., Mah, S., Dhaliwal, H., Reid, A., Pringsheim, T., Dykeman, J., and Gallagher, C. (2016). The international incidence of traumatic brain injury: a systematic review and meta-analysis. Can. J. Neurol. Soc. 43, 774–785.
2. Gorrie, C., Oakes, S., Duflou, J., Blumbergs, P., and Waite, P.M. (2002). Axonal injury in children after motor vehicle crashes: extent, distribution, and size of axonal swellings using beta-APP immunohistochemistry. J. Neurotrauma 19, 1171–1182.
3. Babikian, T., Merkley, T., Savage, R.C., Giza, C.C., and Levin, H. (2015). Chronic aspects of pediatric traumatic brain injury: review of the literature. J. Neurotrauma 32, 1849–1860.
4. Babikian, T., and Asarnow, R. (2009). Neurocognitive outcomes and recovery after pediatric TBI: meta-analytic review of the literature. Neuropsychology 23, 283–296.
5. Akpinar, E., Koroglu, M., and Ptak, T. (2007). Diffusion tensor MR imaging in pediatric head trauma. J. Comput. Assist. Tomogr. 31, 657–661.
6. Ashwal, S., Tong, K.A., Ghosh, N., Bartnik-Olson, B., and Holshouser, B.A. (2014). Application of advanced neuroimaging modalities in pediatric traumatic brain injury. J. Child Neurol. 29, 1704–1717.
7. Wilde, E.A., Chu, Z., Bigler, E.D., Hunter, J.V., Fearing, M.A., Hanten, G., Newsome, M.R., Scheibel, R.S., Li, X., and Levin, H.S. (2006). Diffusion tensor imaging in the corpus callosum in children after moderate to severe traumatic brain injury. J. Neurotrauma 23, 1412–1426.
8. Dennis, E.L., Jin, Y., Villalon-Reina, J.E., Zhan, L., Kernan, C.L., Babikian, T., Mink, R.B., Babbitt, C.J., Johnson, J.L., Giza, C.C., Thompson, P.M., and Asarnow, R.F. (2015). White matter disruption in moderate/severe pediatric traumatic brain injury: advanced tract-based analyses. NeuroImage Clin. 7, 493–505.
9. Dennis, E.L., Hua, X., Villalon-Reina, J., Moran, L.M., Kernan, C., Babikian, T., Mink, R., Babbitt, C., Johnson, J., Giza, C.C., Thompson, P.M., and Asarnow, R.F. (2016). Tensor-based morphometry reveals volumetric deficits in moderate-severe pediatric traumatic brain injury. J. Neurotrauma 33, 840–852.
10. Croall, I., Smith, F.E., and Blamire, A.M. (2015). Magnetic resonance spectroscopy for traumatic brain injury. Top. Magn. Reson. Imaging 24, 267–274.
11. Nordengen, K., Heuser, C., Rinholm, J.E., Matalon, R., and Gundersen, V. (2015). Localisation of n-acetylaspartate in oligodendrocytes/myelin. Brain Struct. Funct. 220, 899–917.
12. McKenna, M.C., Scafidi, S., and Robertson, C.L. (2015). Metabolic alterations in developing brain after injury: knowns and unknowns. Neurochem. Res. 40, 2527–2543.
13. Ashwal, S., Holshouser, B.A., Shu, S.K., Simmons, P.L., Perkin, R.M., Tomasi, L.G., Knierim, D.S., Sheridan, C., Craig, K., Andrews, G.H., and Hinshaw, D.B. (2000). Predictive value of proton magnetic resonance spectroscopy in pediatric closed head injury. Pediatr. Neurol. 23, 114–125.
14. Hoon, A.H., Jr. and Melhem, E.R. (2000). Neuroimaging: applications in disorders of early brain development. J. Dev. Behav. Pediatr. 21, 291–302.
15. Ashwal, S., Holshouser, B.A., and Tong, K.A. (2006). Use of advanced neuroimaging techniques in the evaluation of pediatric traumatic brain injury. Dev. Neurosci. 28, 309–326.
16. Babikian, T., Freier, M.C., Ashwal, S., Riggs, M.L., Burley, T., and Holshouser, B.A. (2006). MR spectroscopy: predicting long-term neuropsychological outcome following pediatric TBI. J. Magn. Reson. Imaging 24, 801–811.
17. Yeo, R.A., Phillips, J.P., Jung, R.E., Brown, A.J., Campbell, R.C., and Brooks, W.M. (2006). Magnetic resonance spectroscopy detects brain injury and predicts cognitive functioning in children with brain injuries. J. Neurotrauma 23, 1427–1435.
18. Babikian, T., Marion, S.D., Copeland, S., Alger, J.R., O'Neill, J., Cazalis, F., Mink, R., Giza, C.C., Vu, J.A., Hilleary, S.M., Kernan, C.L., Newman, N., and Asarnow, R.F. (2010). Metabolic levels in the corpus callosum and their structural and behavioral correlates after moderate to severe pediatric TBI. J. Neurotrauma 27, 473–481.
19. Parry, L., Shores, A., Rae, C., Kemp, A., Waugh, M.C., Chaseling, R., and Joy, P. (2004). An investigation of neuronal integrity in severe paediatric traumatic brain injury. Child Neuropsychol. 10, 248–261.
20. Walz, N.C., Cecil, K.M., Wade, S.L., and Michaud, L.J. (2008). Late proton magnetic resonance spectroscopy following traumatic brain injury during early childhood: relationship with neurobehavioral outcomes. J. Neurotrauma 25, 94–103.
21. Govind, V., Gold, S., Kaliannan, K., Saigal, G., Falcone, S., Arheart, K.L., Harris, L., Jagid, J., and Maudsley, A.A. (2010). Whole-brain proton mr spectroscopic imaging of mild-to-moderate traumatic brain injury and correlation with neuropsychological deficits. J. Neurotrauma 27, 483–496.
22. Govindaraju, V., Gauger, G.E., Manley, G.T., Ebel, A., Meeker, M., and Maudsley, A.A. (2004). Volumetric proton spectroscopic imaging of mild traumatic brain injury. AJNR Am. J. Neuroradiol. 25, 730–737.
23. Maudsley, A.A., Govind, V., Levin, B., Saigal, G., Harris, L., and Sheriff, S. (2015). Distributions of magnetic resonance diffusion and spectroscopy measures with traumatic brain injury. J. Neurotrauma 32, 1056–1063.
24. Ellis, M.U., DeBoard Marion, S., McArthur, D.L., Babikian, T., Giza, C., Kernan, C.L., Newman, N., Moran, L., Akarakian, R., Houshiarnejad, A., Mink, R., Johnson, J., Babbitt, C.J., Olsen, A., and Asarnow, R.F. (2016). The UCLA study of children with moderate-to-severe traumatic brain injury: event-related potential measure of interhemispheric transfer time. J. Neurotrauma 33, 990–996.
25. Dennis, E.L., Ellis, M.U., Marion, S.D., Jin, Y., Moran, L., Olsen, A., Kernan, C., Babikian, T., Mink, R., Babbitt, C., Johnson, J., Giza, C.C., Thompson, P.M., and Asarnow, R.F. (2015). Callosal function in pediatric traumatic brain injury linked to disrupted white matter integrity. J. Neurosci. 35, 10202–10211.
26. Dennis, E.L., Rashid, F., Ellis, M.U., Babikian, T., Vlasova, R.M., Villalon-Reina, J.E., Jin, Y., Olsen, A., Mink, R., Babbitt, C., Johnson, J., Giza, C.C., Thompson, P.M., and Asarnow, R.F. (2017). Diverging white matter trajectories in children after traumatic brain injury: The RAPBI study. Neurology 88, 1392–1399.
27. Moran, L.M., Babikian, T., Del Piero, L., Ellis, M.U., Kernan, C.L., Newman, N., Giza, C.C., Mink, R., Johnson, J., Babbitt, C., and Asarnow, R. (2016). The UCLA study of predictors of cognitive functioning following moderate/severe pediatric traumatic brain injury. J. Int. Neuropsychol. Soc. 22, 512–519.

28. Larson, E.B. and Brown, W.S. (1997). Bilateral field interactions, hemispheric specialization and evoked potential interhemispheric transmission time. Neuropsychologia 35, 573–581.
29. Sabati, M., Sheriff, S., Gu, M., Wei, J., Zhu, H., Barker, P.B., Spielman, D.M., Alger, J.R., and Maudsley, A.A. (2015). Multivendor implementation and comparison of volumetric whole-brain echo-planar MR spectroscopic imaging. Magn. Reson. Med. 74, 1209–1220.
30. Maudsley, A.A., Darkazanli, A., Alger, J.R., Hall, L.O., Schuff, N., Studholme, C., Yu, Y., Ebel, A., Frew, A., Goldgof, D., Gu, Y., Pagare, R., Rousseau, F., Sivasankaran, K., Soher, B.J., Weber, P., Young, K., and Zhu, X. (2006). Comprehensive processing, display and analysis for in vivo MR spectroscopic imaging. NMR Biomed. 19, 492–503.
31. Collins, D.L., Zijdenbos, A.P., Kollokian, V., Sled, J.G., Kabani, N.J., Holmes, C.J., and Evans, A.C. (1998). Design and construction of a realistic digital brain phantom. IEEE Trans. Med. Imaging 17, 463–468.
32. Maudsley, A.A., Domenig, C., Govind, V., Darkazanli, A., Studholme, C., Arheart, K., and Bloomer, C. (2009). Mapping of brain metabolite distributions by volumetric proton MR spectroscopic imaging (MRSI). Magn. Reson. Med. 61, 548–559.

Address correspondence to:
Talin Babikian, PhD
UCLA Semel Institute
760 Westwood Plaza, Room 47-438B
Los Angeles, CA 90095

E-mail: tbabikian@mednet.ucla.edu